EXPERIMENTAL VALIDATION OF CIRCULAR NEAR-FIELD TO FAR-FIELD TRANSFORMATION IN ACOUSTIC TANK EXPERIMENT

Anatoli Tsinovoy[a], Adva Bar-Am[a], Matan Kahanov[a]

[a] Rafael Advanced Defense Systems Ltd., POB 2250(19), Haifa, 3102102 Israel

Anatoli Tsinovoy, Rafael Advanced Defense Systems Ltd., POB 2250(19), Haifa, 3102102 Israel, Fax: +972-733355895
E-mail: anatolt@rafael.co.il

Abstract: *The mono-static target echo strength of a system of two Tungsten-Carbide spheres is measured as a function of azimuth aspect angle. To obtain an estimate of the far-field scattering we apply the Circular Near-Field to Far-Field Transformation (CNFFFT) on near-field measurements. A direct measurement of the far-field scattering was also performed, and used to validate the CNFFFT estimate. At first only partial agreement was achieved. The discrepancy was found to be due to the echoes from the apparatus used to hold and rotate the two spheres. A Fourier-imaging technique allowed us to filter out the unwanted echoes from both the direct and the transformed measurements. The imaging was implemented purely in the r-φ domain, thus avoiding the Cartesian interpolation artefacts common to such processing. Excellent agreement between the two measurements was achieved following removal of the unwanted echoes. A comparison with the theory of scattering from two interacting hard spheres was made and adequate agreement was observed.*

Keywords: *Target echo strength; near-field-to-far-field transformation; sonar imaging*

1. INTRODUCTION

Knowledge of the acoustic target echo strength (TES) of underwater bodies is essential for many underwater applications. TES measurements in a controlled laboratory setting are very rarely possible as direct measurements of the far-field scattering require distances attainable only with at-sea measurements. Measurements of the far-field scattering at-sea involve large distances, and correspondingly large experimental uncertainties.

Thus, a solution is required to enable determination of the far-field TES from acoustic near-field scattering measurements, be they at-sea, or at an acoustic tank facility. In this work we demonstrate the Circular Near-Field to Far-Field Transformation (CNFFFT), also known as Wavenumber Migration [1]. This approach is applicable for planar monostatic measurements. Due to the essentially planar propagation of acoustic energy in the ocean even at moderate distances, the TES is of most interest as a function of the azimuth aspect angle, φ, at elevation $\theta=\pi/2$.

The aim of this study is to demonstrate the inference of monostatic TES of a system of two Tungsten-Carbide (TC) spheres as a function of φ at $\theta=\pi/2$ from near-field scattering measurements over that same angular range performed at Rafael's Underwater Test Facility. Results are validated by comparison to far-field measurements and theory.

2. EXPERIMENTAL SETUP

The monostatic TES of a system of two TC spheres was measured. The two spheres were of diameter D=38 mm, and were held a distance d=18 cm apart using a custom-made 3D-printed plastic apparatus. The system and transducer were both lowered to a depth of about 5 m (See Fig. 1). Alignment of the system under test and transducer was performed by finding the orientation and depth at which the measured echo was at a maximum. The transducer employed had a resonance frequency of 85 kHz, and was used both as transmitter and as hydrophone, with the aid of a T/R switch. At the measurement distances employed, the target spanned at most 10^{o} of the beam-pattern, over which there is no more than 0.5 dB variation. The waveform used in the actual measurements was a 20 cycle pulse at f_c=80 kHz windowed by a Tukey window function (r=0.5).

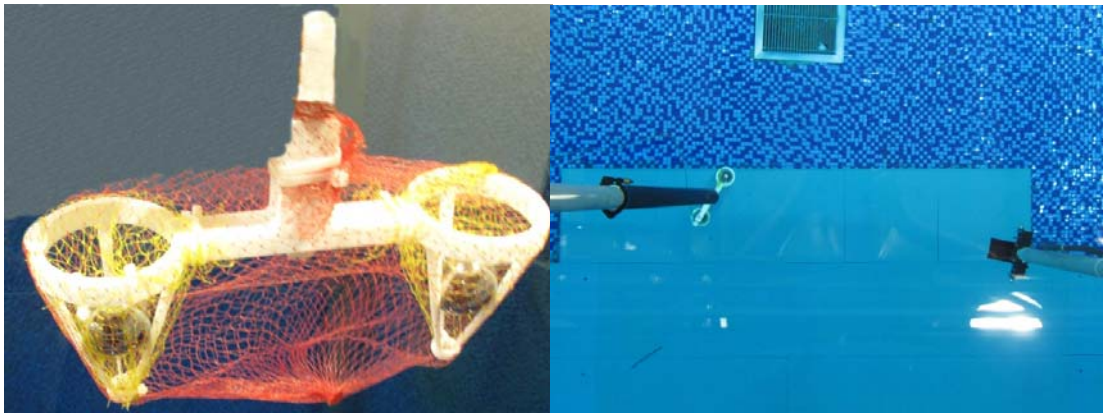

Fig.1: (left) The two TC spheres (In 3D-printed holder). (right) The two spheres immersed in the pool, connected to a special rod made of polyurethane, with the measurement transducer positioned facing the system.

The quantity of interest in the measurement is the ratio of the received echo pressure to the transmitted pressure amplitude. Extraction of this information from the received echo voltage requires knowledge of the transmitted waveform and the product of the transducer's transmit response and receive response. A calibration procedure was carried out where the echo from a calibration target of known TES (A single small hard sphere) was measured. The waveform used for calibration was a chirp spanning the frequency range 40 kHz-120 kHz. The calibration followed the procedure presented in [2].

3. CIRCULAR NEAR-FIELD TO FAR-FIELD TRANSFORMATION

In this chapter we give a brief overview of the circular near-field to far-field transformation algorithm based on [1]. The measurement plane is xy, utilizing cylindrical coordinates, $\vec{r} = (\rho\cos\theta \quad \rho\sin\theta \quad z)$, $\vec{\rho} = (\rho\cos\theta \quad \rho\sin\theta)$. We denote the acoustic wavelength by λ and the acoustic wavenumber by $k = 2\pi/\lambda$.

We assume the target can be adequately described by a single-scattering model, and that we measure at R_0, in the far-field with respect to the z axis: $z'^2/2\lambda R_0 < 1$. We model the monostatic scattering using the target's surface reflectivity function, $\sigma(\vec{\rho})$, that is related to the more familiar volume reflectivity function, $\gamma(\vec{r})$, by $\sigma(\vec{\rho}) = \int_\Omega dz'\,\gamma(\vec{\rho}', z')$.

In addition we assume that our transducer is isotropic over the extent of the target. Then the following model applies to the monostatic echo for a transducer positioned at $\vec{R}$ for a CW input at unit amplitude. In our circular measurement geometry, $\vec{R} = R_0(\cos\varphi \quad \sin\varphi \quad 0)$, for brevity, we denote $\vec{\rho}_0 = R_0(\cos\varphi \quad \sin\varphi)$.

$$p_{rec}(\vec{R},k) = \iint_{\Omega'} dS\,\sigma(\vec{\rho}', z')\frac{e^{2ik|\vec{\rho}_0 - \vec{\rho}'|}}{|\vec{\rho}_0 - \vec{\rho}'|^2} \tag{1}$$

Where the integration domain, Ω', is the extent of the target in the measurement plane.

The following relationship holds between the TES, $S(\varphi,k) = \lim_{R_0\to\infty} R_0^2 e^{-2ikR_0} p_{rec}(\vec{R},k)$, and the surface reflectivity function $\sigma(\vec{\rho})$:

$$S(\varphi,k) = \iint_{\Omega'} dS\,\sigma(\vec{\rho}')e^{2ik\rho'\cos(\varphi-\varphi')} \tag{2}$$

Applying the fractional order derivative $(i/2\, d/dk)^{3/2}$ to Eq. 1 provides us with an auxiliary field, $q_{rec}(\vec{R},k) \equiv (i/2\, d/dk)^{3/2} p_{rec}(\vec{r},k)$ corresponding to one-way propagation at frequency 2k. A simple relationship between $q_{rec}(R_0,\varphi,k)$ and the TES can be derived:

$$S(\varphi,k) = \frac{1}{2\pi}\sum_{n=-\infty}^{\infty} e^{in\varphi}\left(\frac{i^n}{\sqrt{ik\pi}H_n^{(2)}(2kR_0)}\right)\left(\int_0^{2\pi} d\psi e^{-in\psi} q_{rec}(R_0,\psi,k)\right) \tag{3}$$

The sum and integral in this formula can be implemented using 1D (I)FFT operations. For targets large enough so that the beam-pattern can no longer be considered constant, a beam-pattern correction is applicable [3].

In contrast with previous work, we worked with a single finite rather than many CW measurements. This required the application of the fractional order derivative using the Grunwald-Letnikov integral formulation in order to receive a result that is both band-limited and reasonably localized in time.

The Fourier-relationship in Eq. 2 can be inverted for the surface reflectivity function $\sigma(\vec{\rho})$. This is usually done by interpolating $S(\varphi,k)$ to a Cartesian grid $S(k_x,k_y)$ and performing a 2D DFT. This process creates artefacts in the resulting space-domain function unless a very fine interpolation grid is used. We implemented a Bessel-Fourier transformation from $S(\varphi,k)$ directly to $\sigma(\rho,\theta)$ using the angular DFT and a Bessel integral transform for the radial coordinate. Interpolation to (x,y) was used only for display purposes. This avoids the artefacts, and allows for exact processing of $\sigma(\rho,\theta)$.

4. RESULTS

The measurements were carried out at intervals of 1°. This is fine enough as $\Delta\varphi_{\min} = {}^{360^o}\!/_{2kd+10} \approx 2^o$ is the Nyquist sample rate for our system. The near-field distance for our system is 108 cm. The near-field measurements were carried out at R_0=96 cm, and the far-field measurements were carried out at R_0=242 cm.

Comparison to theory was carried out using a model for the TES of a system of two hard spheres [4]. The TC spheres used do not show any prominent resonances over the frequency range measured, and so the assumption of rigidity is well-fulfilled. The calibration target used was a TC sphere of diameter D=24 mm. It shows one weak resonance over the measured frequencies, and so we are assured that our calibration is not sensitive to small variations in its material parameters [2].

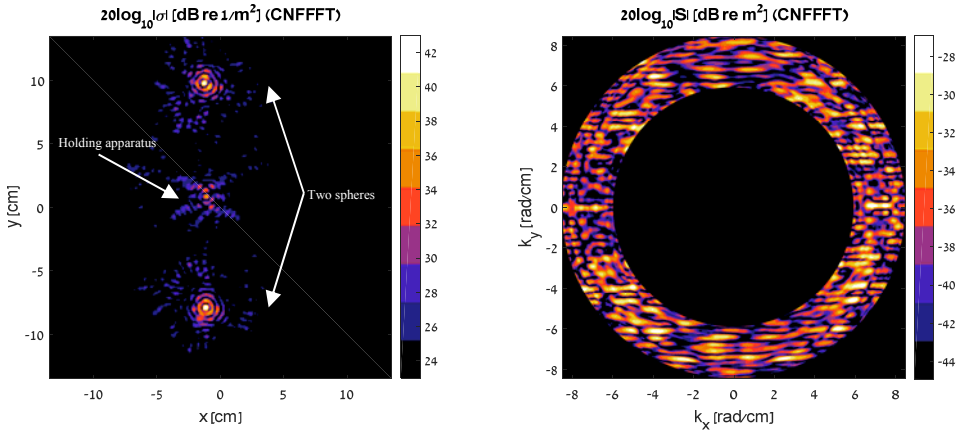

Fig. 2: (left) $\sigma(x,y)$ corresponding to $S(k_x,k_y)$ as found by Bessel-Fourier transform. (right) $S(k_x,k_y)$ according to CNFFFT. The two spheres are clearly visible, as is a third scattering centre associated with the holding apparatus.

In Fig. 2 the results of the CNFFFT algorithm are presented in both frequency-domain and space-domain. The holder apparatus (Identifiable as the scattering centre near the

origin in the space-domain display) is then removed with a spatial mask, and the result is Fourier-Bessel transformed back to frequency-domain. This is done for both the results of the CNFFFT and the direct far-field measurement of the TES. Comparison between the two results is shown in Fig. 3.

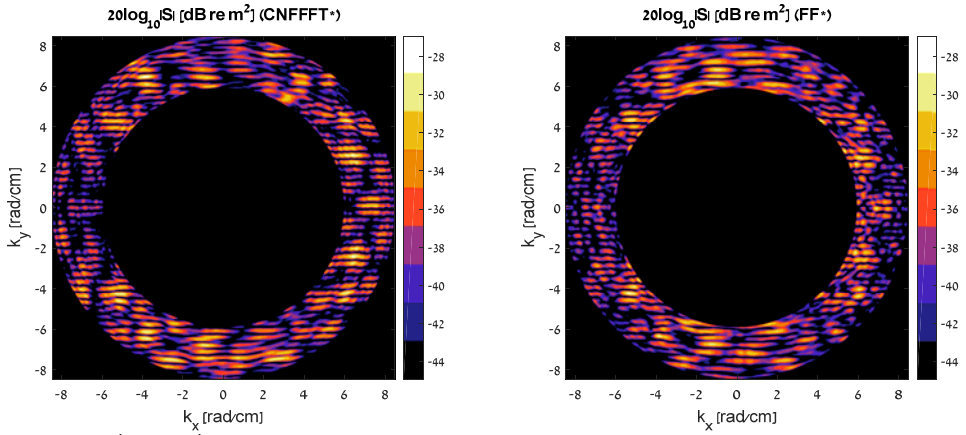

Fig.3: (left) $S(k_x, k_y)$ according to CNFFFT with the holding apparatus masked in space-domain. (right) $S(k_x, k_y)$ measured in the far-field with the holding apparatus masked in space-domain.

Excellent agreement is observed between the CNFFFT results and the direct far-field measurement, after removal of the reflections associated with the holding apparatus. It is of interest that comparison prior to this masking process is much less favourable. This is due to the holding apparatus' (Long cylinder) length along the z axis, which breaks the planarity assumption of the CNFFFT.

A comparison with theory can also be made, shown in Fig. 4.

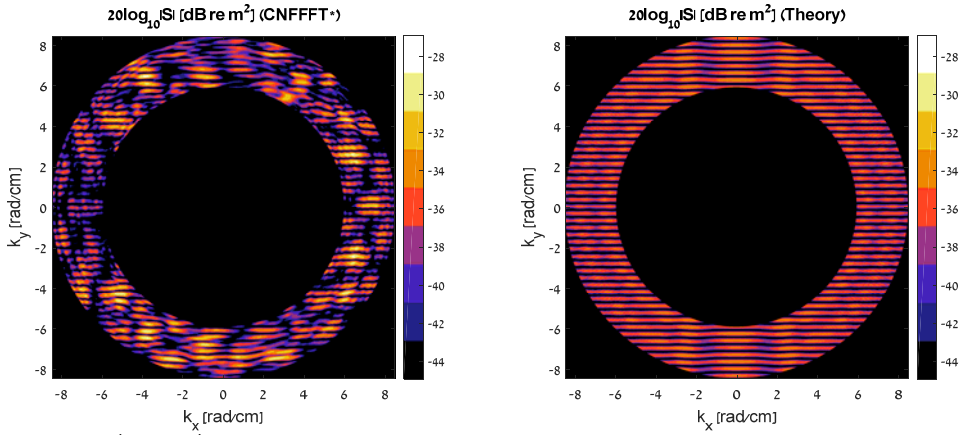

Fig.4: (left) $S(k_x, k_y)$ according to CNFFFT with the holding apparatus masked in space-domain. (right) $S(k_x, k_y)$ according to theory.

Good agreement between theory and experiment can be observed, both in terms of amplitude and in terms of the structure along k_y, although there is clear disagreement both in the peak TES observed (On the order of 5 dB) and in the structure evident in the measured data but absent from our theoretical model.

5. SUMMARY AND CONCLUSIONS

The CNFFFT has been briefly introduced, and demonstrated for a system of two TC spheres. The measured echo from 1D near-field measurements of the system was used to infer the TES as a function of azimuth angle φ and elevation $\theta = \pi/2$. The CNFFFT involves a fractional order derivative that has been implemented in a novel way.

A Fourier-Bessel transformation was implemented for acoustic imaging of the system. This allowed the unwanted scattering centre associated with the holding apparatus to be resolved from the system under test and masked out in space-domain.

After spatial masking of the unwanted scattering centre, excellent agreement was observed between the CNFFFT TES estimate and direct far-field measurement of the TES. Satisfactory agreement between both experimental results and theory was observed. Taking into account the excellent agreement between CNFFFT and true far-field results seen in Fig. 3, we conclude that the discrepancy between theory and experiment is due to the 3D-printed plastic holder used, whose echo could not be separated from the actual TC spheres.

We have thus shown that the CNFFFT with Fourier-Bessel imaging for removal of unwanted scattering centres provides a good method for evaluating the monostatic TES of a thin system.

6. ACKNOWLEDGEMENTS

The authors are grateful to the following people from the Israeli Underwater Acoustics Excellency Centre, Rafael's David Institute, Haifa, Israel, for their assistance on this project: Yair Dimant, Gilbert Abutbol, and Yotam Gershon.

REFERENCES

[1] **B. E. Fischer**, On the Use of Wavenumber Migration for Linear SAR Image Formation and Near-Field to Far-Field RCS Transformation, In *Proceedings of the 23rd Annual Meeting of the Antenna Measurement Techniques Association (AMTA '01)*, 4, pp. 117-122, 2001.

[2] **T. K. Stanton, D. Chu**, Calibration of broadband active acoustic systems using a single standard spherical target, *J. Acoust. Soc. Am.*, 124 (1), pp. 128-136, 2008.

[3] **I. J. LaHaie, S. A. Rice**, Antenna-Pattern Correction for Near-Field-to-Far-Field RCS Transformation of 1D Linear SAR Measurements, *IEEE Antennas and Propagation*, 46 (4), pp. 177-183, 2004.

[4] **G.C. Gaunaurd, H. Huang**, Acoustic Scattering by a Pair of Spheres, *J. Acoust. Soc. Am.*, 98 (1), pp. 642-651, 1995.